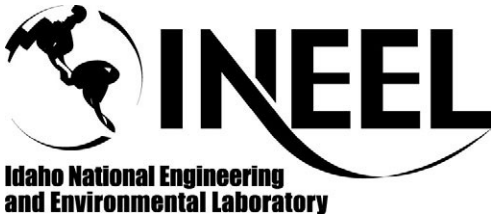

INEEL/CON-04-02407
PREPRINT

Numerical Simulation And Experimental Characterization Of A Binary Aluminum Alloy Spray – Application To The Spray Rolling Process

S. B. Johnson
J. P. Delplanque
Y. Lin
Y. Zhou
E. J. Lavernia
K. M. McHugh

February 13-17, 2005

134th Annual Meeting And Exhibition – The Minerals, Metals & Materials Society (TMS) 2005

TMS (The Minerals, Metals & Materials Society)

Numerical Simulation and Experimental Characterization of a Binary Aluminum Alloy Spray – Application to the Spray Rolling Process

S. B. Johnson[1], J.-P Delplanque[1], Y. Lin[2], Y. Zhou[2], E. J. Lavernia[2], K. M. McHugh[3]

[1]Engineering Division, Colorado School of Mines; Golden, CO, 80401, USA
[2]Department of Chemical Engineering and Materials Science; University of California, Davis, CA, 95616, USA
[3]Industrial and Material Technologies Department; Idaho National Engineering and Environmental Laboratory, Idaho Falls, Idaho, 83415, USA

Keywords: Spray, Aluminum, Simulation

Abstract

A stochastic, droplet-resolved model has been developed to describe the behavior of a binary aluminum alloy spray during the spray-rolling process. In this process, a molten aluminum alloy is atomized and the resulting spray is deposited on the rolls of a twin-roll caster to produce aluminum strip. The one-way coupled spray model allows the prediction of spray characteristics such as enthalpy and solid fraction, and their distribution between the nozzle and the deposition surface. This paper outlines the model development and compares the predicted spray dynamics to PDI measurements performed in a controlled configuration. Predicted and measured droplet velocity and size distributions are presented for two points along the spray centerline along with predicted spray averaged specific enthalpy and solid fraction curves.

Introduction

Sprays are an integral part of many industrial processes. Spray systems are complex, and involve a wide range of length and time scales. The large disparity of scales makes reliable and computationally efficient simulations challenging, but beneficial because of the wide range of applicability.

Spray rolling is one such industrial process that utilizes a spray system. Spray rolling combines spray deposition and twin-roll casting into a highly efficient technique for the production of aluminum strip [1]. First, molten aluminum is atomized with a high velocity transverse jet. The resulting droplets are then quenched in-flight to a partially solidified state, and deposited in the nip of a rolling mill. While still highly formable, the deposited material is consolidated into a strip through the rolling process.

The spray-rolling process is an emerging technology, and therefore, not fully understood. To enhance the understanding of spray rolling, subprocess models are currently being developed and integrated into a global model for the overall spray-rolling process. One such subprocess model, is the spray model outlined herein. This spray model uses a mixed Lagrangian/Eulerian method whereby computational particles representing the

spray are tracked in a Lagrangian manner through an Eulerian flow field. Due to the complex shape of the spray-rolling chamber, three dimensional flow-field simulation and particle tracking are required. To reduce computational costs, the dispersed and continuous phases are coupled in a one-way manner, neglecting the influence of the dispersed phase on the continuous phase momentum and energy conservation equations, which is valid for dilute sprays.

A preliminary investigation of the reliability of this model is presented. In this investigation droplet velocity and diameter distributions are compared to available data obtained using phase doppler interferometry (PDI) at two locations along the spray axis.

Experimental Methods

While the spray model discussed herein is designed with applicability to spray rolling, a spray rolling chamber has not yet been fitted with the diagnostic tools necessary to characterize the spray within it. It is therefore necessary to use other facilities with appropiate diagnostic tools and a controlled environment for a comparison of the spray model [2].

The spray forming facility used in the present experiments is comprised of a spray chamber (1.06 m in diameter and 2.5 m in height), atomizer unit, induction unit, substrate for depositon, gas manifold, gas exhaust and a power collection system. The melt is allowed to fall through a liquid metal delivery nozzle by lifting the stopper inside the crucible, and atomized into a distribution of micrometer-sized droplets using nitrogen gas. To reduce oxidation, the experiments were conducted inside an environmental chamber, which was evacuated and backfilled with nitrogen.

A phase Doppler interferometer (Aerometrics RSA, Sunnyvale, CA, USA) was utilized to characterize, *i*n-situ, the metal spray behavior, droplet size and velocity simultaneously. Phase Doppler interferometry is a single droplet counting technigue which can, in principle, be used for on-line measurement of the atomized powder size and velocity. The technique is an extension of laser Doppler anemometry, in which two laser beams are intersected at the region of interest, forming an interferometric sampling volume.

Spray Model

The spray model outlined below couples a three-dimensional flow field simulation to particle tracking and heat transfer models. The coupling is done in a one way manner to preserve computational efficiency. Heat transfer and solidification is modeled with a multi-stage lumped parameter approach, which includes the influence of rapid solidification.

Continuous Phase Simulation

The continuous phase in the spray system is modeled using numerical simulation of the Navier-Stokes and energy equations. The current results are calculated using a commercial CFD code, CFD-ACE (CFDRC, Huntsville, AL). The continuous phase conservation equations are solved without coupling to the dispersed phase momentum, heat and mass transfer. This procedure eliminates the costly iterations between continuous and dispersed phase calculations, and allows the simulation results to be calculated once and used as an

interpolation library for repeated dispersed phase calculations. However, one-way coupling is only valid for dilute sprays and suffers from some inaccuracy near the atomization region.

Spray Discretization

To model the spray as a whole, it is not practical to calculate the trajectories of every droplet within the spray. A more pragmatic approach is to discretize the spray into computational particles, for which the trajectories and thermal histories are calculated. Those trajectories are integrated downstream to reconstruct the spray as a whole. To this end, the spray is modeled with distributions for the initial droplet size and velocity. Computational particles are sampled randomly from these distributions and their trajectories and thermal histories are calculated. For the current study, the droplet size distributions ($g_D(D)$) is modeled with a log normal distribution,

$$g_D(D) = \frac{1}{\sqrt{2\pi}\ln\sigma_D}\exp\left[-\frac{(\ln D - \ln D_m)^2}{2\ln {\sigma_D}^2}\right], \tag{1}$$

the droplet initial speed ($g_c(c)$) of the droplet is modeled with a normal distribution,

$$g_c(c) = \frac{1}{\sqrt{2\pi}\sigma_c}\exp\left[-\frac{(c-\mu_c)^2}{2\sigma^2}\right] \tag{2}$$

and the circumferential and azimuthal spray angles are modeled with uniform distributions. The size, speed and angle distributions are modeled as independent from one another.

Particle Momentum

It is necessary to have knowledge of the droplet gas relative velocity, and the particle location for evaluation of the continuous phase properties and to determine the influence of the continuous phase on particle solidification and heat transfer. It is alo necessary to know particle velocities and positions for reintegration of the spray down stream from injection. To these ends, trajectories for computational particles are calculated using a simplified version of the particle equation of motion [3],

$$\frac{d\boldsymbol{V}_d}{dt} = \boldsymbol{g}\left(1-\frac{\rho_g}{\rho_d}\right) + \frac{3}{4D}\frac{\rho_g}{\rho_d}\left\|\boldsymbol{V}_g - \boldsymbol{V}_d\right\|\left(\boldsymbol{V}_g - \boldsymbol{V}_d\right)C_d \tag{3}$$

where $\boldsymbol{V}_d$ is the particle velocity, $\boldsymbol{V}_g$ is the continuous phase velocity at the particle location, ρ_d and ρ_g are the droplet and continuous phase densities, respectively, $\boldsymbol{g}$ is the gravitational acceleration, and C_d is the drag coefficient.

Particle Heat Transfer and Solidification

Grant, Cantor, and Katagerman proposed a model to describe the in-flight solidification of a droplet of a binary alloy (including rapid solidification effects) [4, 5, 6]. This model was later modified by Cai and Lavernia [7] to include radiative cooling. This model breaks the solidification process into five stages: liquid cooling, recalescence, segregated solidification, eutectic solidification, and solid cooling.

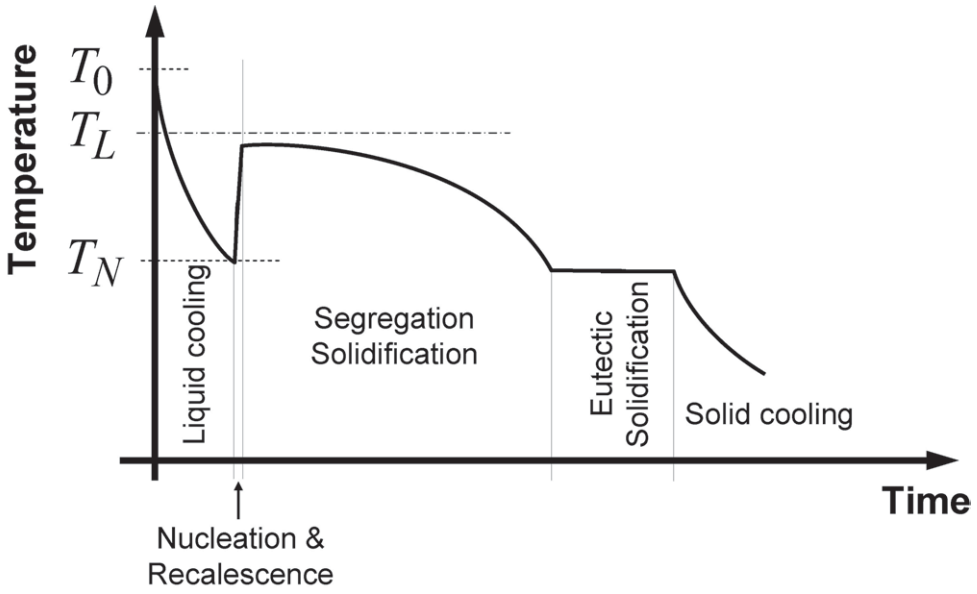

Figure 1: Schematic representation of the droplet solidification stages

As a droplet cools and solidifies, the time rate of change of the droplet total enthalpy (H) is balanced by the rate that energy is transfered to the droplet by convection ($\dot{Q}_{conv}$) and radiation ($\dot{Q}_{rad}$),

$$\frac{dH}{dt} = \dot{Q}_{conv} + \dot{Q}_{rad}. \tag{4}$$

The convective rate of heat transfer is given by the product of the surface area (A), a linear heat transfer coefficient (η) and the difference in temperature between the droplet surface (T_s) and the continuous phase (T_g):

$$\dot{Q}_{conv} = A\eta \left(T_g - T_s\right), \tag{5}$$

where the linear heat transfer coefficient is calculated using the Ranz-Marshall correlation [8]. The radiative rate of heat transfer is given by the product of the surface area, the emissivity at the surface (ϵ), the Stefan-Boltzmann constant (σ_B), and the difference between the surface temperature to the fourth power and the temperature of the evironment (T_e) to the fourth power:

$$\dot{Q}_{rad} = A\epsilon\sigma_B \left(T_e^4 - {T_s}^4\right). \tag{6}$$

The total enthalpy of the droplet is the sum of the enthalpy in the liquid and the enthalpy in the solid, which may be expressed by [9]

$$H = m(1 - f_s)\left[C_{p,\ell}\left(T - T_L\right) + \Delta h_f\right] + m f_s C_{p,s}\left(T - T_L\right) + m h_0, \tag{7}$$

where m is the mass of the droplet, f_s is the solid fraction, Δh_f is the latent heat of fusion, $C_{p,\ell}$ and $C_{p,s}$ are the liquid and solid specific heats, T_L is the liquidus temperature, and h_0 is the specific enthalpy of the solid at the liquidus temperature. During each stage of the solidification process, the rate of change of the total enthalpy is expressed differently according to the relevant processes and phases.

During the liquid cooling stage of the solidification process, there is no solid present and no phase change is occurring. Eliminating the appropriate terms, the rate of change in enthalpy becomes

$$\frac{dH}{dt} = mC_{p,\ell}\frac{dT}{dt}. \tag{8}$$

Once the nucleation temperature (T_N, which is calculated using Hirth's equation [10]) has been reached, rapid solidification occurs and the rate of release of latent heat overwhelms the rate of heat extracted by convection and radiation at the droplet surface. During this stage of solidification the change in total enthalpy is neglected and the post-recalescence solid fraction (f_R) is calculated by assuming that the post-recalescence droplet temperature (T_R) returns to the liquidus temperature [7, 9]. These assumptions lead to the following expression for the post-recalescence solid fraction:

$$f_s = \frac{C_{p,\ell}\left(T_L - T_N\right)}{\Delta h_f}. \tag{9}$$

In the case where the droplet has become hypercooled, the total available latent heat is not sufficient to bring the droplet temperature back up to the liquidus temperature. When this occurs the droplet is assumed to solidify completely during recalescence and the post-recalescence temperature is calculated as

$$T_R = \frac{C_{p,\ell}\left(T_N - T_L\right) + \Delta h_f}{C_{p,s}} + T_L. \tag{10}$$

After recalescence, if the droplet did not experience hypercooling, the droplet undergos a segregated solidification stage. During segregated solidification, both liquid and solid phases are present and heat extraction at the droplet surface is relevant again. This leads to the following expression for the rate of change of total enthalpy:

$$\frac{dH}{dt} = m\frac{d}{dt}\left\{\left(1 - f_s\right)\left[C_{p,\ell}\left(T - T_L\right) + \Delta h_f\right] + C_{p,s}\left(T - T_L\right)\right\} \tag{11}$$

During segregated solidification it is assumed that there is infinite rate diffusion of the solute in the liquid [11], and diffusion in the solid is neglected. With these assumptions and using the Scheil equation [11], the droplet solid fraction may be related to the temperature,

$$f_s = 1 - \left(1 - f_R\right)\left[\frac{T_M - T - R}{T_M - T}\right]^{\frac{k_e - 2}{k_e - 1}}, \tag{12}$$

where T_M is the melting point of the solvent and k_e is the equilibrium partition ratio.

During segregated solidification the concentration of the solute in the liquid increases until the eutectic concentration is reached. At this point the eutectic solidification stage begins. During eutectic solidification the droplet remains at the eutectic solidification temperature (T_E), and the rate of change of the total enthalpy is related to the change in solid fraction

$$\frac{dH}{dt} = m\left[\left(C_{p,s} - C_{p,\ell}\right)\left(T_E - T_L\right) - \Delta h_f\right]\frac{f_s}{dt}. \tag{13}$$

Once the droplet becomes completely solidified, either during the eutectic solidification stage or during recalescence for hypercooled droplets, the solid cooling stage begins. During the solid cooling stage, there is no liquid present in the droplet and no phase change occurs. This leads to the following expression for the rate of change in total enthalpy:

$$\frac{dH}{dt} = mC_{p,s}\frac{dT}{dt}. \tag{14}$$

Equation 14 continues to govern droplet heat transfer through the end of the droplet's flight.

Results and Discussion

Droplet size and velocity distributions where obtained experimentally using the PDI technique for 3003 aluminum alloy with the target substrate located 0.41 m from the atomization nozzle. Distributions were collected for two points along the spray centerline, 0.26 m and 0.31 m from the atomization nozzle. Histograms for the experimental data, shown in Figure 2, show a overall decrease in the axial velocity as the spray approaches the target substrate, as well as an overall decrease in the droplet diameter. While the decrease in the axial velocity may be explained by the influence of the reduced axial velocity of the continuous phase as it approaches the substrate, a mechanism has not yet been identified to explain the changes of the size distribution.

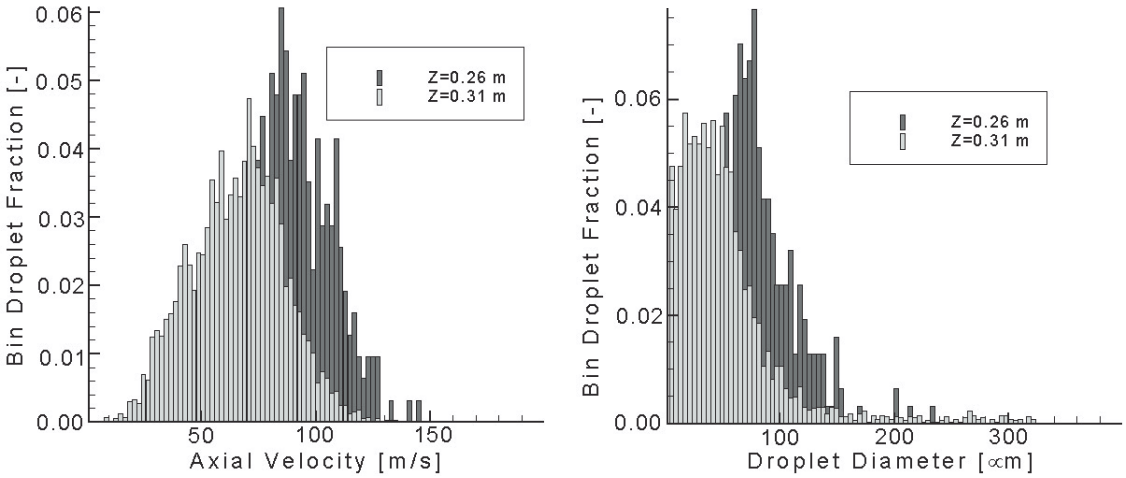

Figure 2: Experimentally measured droplet velocity and size distributions along the spray centerline 0.26 m and 0.31 m from the atomization nozzle.

Simulation results where obtained with estimated parameters for similar operating conditions. The continuous phase flow field was calculated for 250 ms/ nitrogen jet directed towards a solid substrate 0.41 m from the nozzle. For this study 10,000 computational particles were injected into the flow field at the nozzle exit with a spray angle of 20^o, mass median diameter of 100 μm and 100 K superheat. The spray was sampled and the same locations given above for the experimental data, and histograms for the model results are shown in Figure 3. The predicted data also indicates a decrease in the mean axial velocity as the droplets approach the substrate, but the change is less pronounced than in the

experimental data, and there is no significant change in the mean diameter as was seen in the experimental data. There is also a discrepency in the shape of the distributions where the predicted velocity distribution appears to be trucated at high values. The shape of the velocity distribution was found to be sensitive to the input parameters.

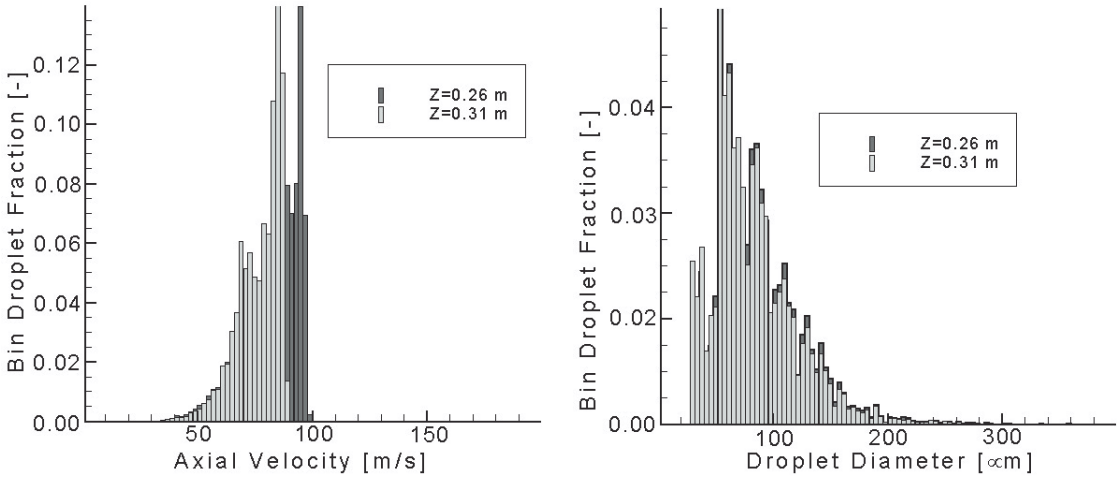

Figure 3: Predicted droplet velocity and size distributions along the spray centerline 0.26 m and 0.31 m from the atomization nozzle.

In addition to the velocity and size data, the current model also predicts the thermal history of individual droplets as well as spray averages. Figure 4 shows the temperature of droplets with various sizes, ranging from 50 μm to 200 μm, as a function of the distance from the atomization nozzle. The results indicated that the smaller droplets will solidify completely at a much shorter distance from the nozzle and will experience a higher degree of undercooling due to a higher cooling rate.

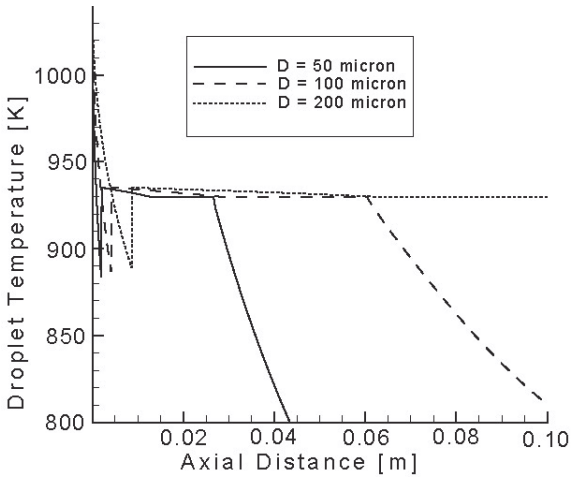

Figure 4: Predicted droplet temperatures as a function of distance from the atomization nozzle for various droplet sizes.

The spray averaged specific enthalpy are shown in Figure 5 as a function of the distance from the atomization nozzle. The results indicate that the spray will reach a solid fraction

of roughly 90% before being deposited onto the target substrate.

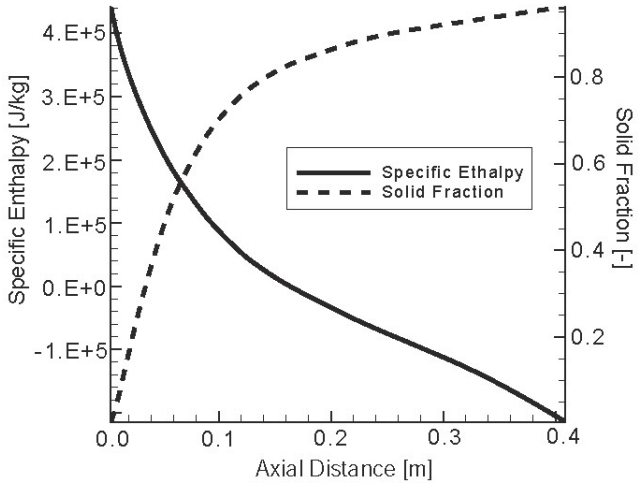

Figure 5: Predicted average spray specific enthalpy and solid fraction as a function of the axial distance from the injection nozzle.

Conclusions

A mixed Lagragian/Eulerian model has been developed to describe the heat transfer and solidification of a binary alloy spray (including the effect of rapid solidification) with application to spray rolling. This model uses a multi-stage approach to model alloy solidification and is one-way coupled to improve computational efficiency. Discrepancies exist between the predicted spray behavior and the experimental data obtained using phase Doppler interferometry. A comparison with a more extensive collection of data is required to fully evaluate the spray model.

Acknowledgements

The financial support of the U.S. DOE, Idaho Operation Office (DE-FC07-00ID13816), U.S. Department of Education GAANN program (P200A000447), the Brown Foundation at the Colorado School of Mines and the Center for Combustion and Environmental Research at the Colorado School of Mines is gratefully acknowledged.

References

[1] K.M. McHugh, J.-P Delplanque, S.B. Johnson, E.J. Lavernia, Y. Zhou, and Y. Lin. Spray rolling aluminum alloy strip. *Materials Science and Engineering A*, In Press, 2004.

[2] Y. Zhou. *An investigation of droplet behavior during spray-based manufacturing processes*. PhD thesis, University of California, Irvine, 1999.

[3] J.-P. Delplanque, E.J. Lavernia, and R.H. Rangel. Analysis of in-flight oxidation during reactive spray atomization and deposition processing of aluminum. *Journal of Heat Transfer*, 122(1):126–132, 2000.

[4] P.S. Grant, B. Cantor, and L. Katerman. Modelling of droplet dynamics and thermal histories during spray forming - i. individual droplet behavior. *Acta Metallurgica et Materialia*, 41(11):3097–3108, 1993.

[5] P.S. Grant, B. Cantor, and L. Katerman. Modelling of droplet dynamics and thermal histories during spray forming - ii. effect of process parameters. *Acta Metallurgica et Materialia*, 41(11):3109–3118, 1993.

[6] P.S. Grant and B. Cantor. Modelling of droplet dynamics and thermal histories during spray forming - iii. analysis of spray solid fraction. *Acta Metallurgica et Materialia*, 43(3):913–921, 1995.

[7] W. Cai and E.J. Lavernia. Modeling porosity during spray forming: Part i. effects of processing parameters. *Metallurgical and Materials Transactions B*, 29B:1085–1096, 1998.

[8] W.E. Ranz and W.R. Marshall. Evaporation from drops (part i). *Chemical Engineering Progress*, 48(3):141–180, 1952.

[9] C.G. Levi and R. Mehrabian. Heat flow during rapid solidification of undercooled metal droplets. *Metallurgical Transactions A - Physical Metallurgy and Materials Science*, 13A(2):221–234, 1982.

[10] J.P. Hirth. Nucleation, undercooling and homogeneous structures in rapidly solidified powders. *Metallurgical Transactions A*, 9A:401–404, 1978.

[11] Merton C. Flemings. *Solidification Processing*. McGraw-Hill, 1974.